

---

# Learning Neural Networks with Adaptive Regularization

---

Anonymous Author(s)

Affiliation

Address

email

## Abstract

1        Feed-forward neural networks can be understood as a combination of an interme-  
2        diate representation and a linear hypothesis. While most previous works aim to  
3        diversify the representations, we explore the complementary direction by perform-  
4        ing an adaptive and data-dependent regularization motivated by the empirical Bayes  
5        method. Specifically, we propose to construct a matrix-variate normal prior (on  
6        weights) whose covariance matrix has a Kronecker product structure. This structure  
7        is designed to capture the correlations in neurons through backpropagation. Under  
8        the assumption of this Kronecker factorization, the prior encourages neurons to  
9        borrow statistical strength from one another. Hence, it leads to an adaptive and  
10       data-dependent regularization when training networks on small datasets. To opti-  
11       mize the model, we present an efficient block coordinate descent algorithm with  
12       analytical solutions. Empirically, we demonstrate that the proposed method helps  
13       networks converge to local optima with smaller stable ranks and spectral norms.  
14       These properties suggest better generalizations and we present empirical results  
15       to support this expectation. We also verify the effectiveness of the approach on  
16       multiclass classification and multitask regression problems with various network  
17       structures.

## 18 1 Introduction

19        Although deep neural networks have been widely applied in various domains [19, 25, 29], usually its  
20        parameters are learned via the principle of maximum likelihood, hence its success crucially hinges  
21        on the availability of large scale datasets. When training rich models on small datasets, explicit  
22        regularization techniques are crucial to alleviate overfitting. Previous works have explored various  
23        regularization [42] and data augmentation [19, 41] techniques to learn diversified representations.  
24        In this paper, we look into an alternative direction by proposing an adaptive and data-dependent  
25        regularization method to encourage neurons of the same layer to share statistical strength. The goal of  
26        our method is to prevent overfitting when training (large) networks on small dataset. Our key insight  
27        stems from the famous argument by Efron [8] in the literature of the empirical Bayes method: *It is*  
28        *beneficial to learn from the experience of others*. From an algorithmic perspective, we argue that the  
29        connection weights of neurons in the same layer (row/column vectors of the weight matrix) will be  
30        correlated with each other through the backpropagation learning. Hence, by learning the correlations  
31        of the weight matrix, a neuron can “borrow statistical strength” from other neurons in the same layer.

32        As an illustrating example, consider a simple setting where the input  $\mathbf{x} \in \mathbb{R}^d$  is fully connected to a  
33        hidden layer  $\mathbf{h} \in \mathbb{R}^p$ , which is further fully connected to the single output  $\hat{y} \in \mathbb{R}$ . Let  $\sigma(\cdot)$  be the  
34        nonlinear activation function, e.g., ReLU [36],  $W \in \mathbb{R}^{p \times d}$  be the connection matrix between the  
35        input layer and the hidden layer, and  $\mathbf{a} \in \mathbb{R}^p$  be the vector connecting the output and the hidden layer.  
36        Without loss of generality, ignoring the bias term in each layer, we have:  $\hat{y} = \mathbf{a}^T \mathbf{h}$ ,  $\mathbf{h} = \sigma(W\mathbf{x})$ .  
37        Consider using the usual  $\ell_2$  loss function  $\ell(\hat{y}, y) = \frac{1}{2}|\hat{y} - y|^2$  and take the derivative of  $\ell(\hat{y}, y)$  w.r.t.

38  $W$ . We obtain the update formula in backpropagation as  $W \leftarrow W - \alpha(\hat{y} - y)(\mathbf{a} \circ \mathbf{h}') \mathbf{x}^T$ , where  
 39  $\mathbf{h}'$  is the componentwise derivative of  $\mathbf{h}$  w.r.t. its input argument, and  $\alpha > 0$  is the learning rate.  
 40 Realize that  $(\mathbf{a} \circ \mathbf{h}') \mathbf{x}^T$  is a rank 1 matrix, and the component of  $\mathbf{h}'$  is either 0 or 1. Hence, the  
 41 update for each row vector of  $W$  is linearly proportional to  $\mathbf{x}$ . Note that the observation holds for any  
 42 input pair  $(\mathbf{x}, y)$ , so the update formula implies that the row vectors of  $W$  are correlated with each  
 43 other. Although in this example we only discuss a one-hidden-layer network, it is straightforward to  
 44 verify that the gradient update formula for general feed-forward networks admits the same rank one  
 45 structure. The above observation leads us to the following question:

46 *Can we define a prior distribution over  $W$  that captures the correlations through*  
 47 *the learning process for better generalization?*

48 **Our Contributions.** To answer the above question, we develop an adaptive regularization method for  
 49 neural nets inspired by the empirical Bayes method. Motivated by the example above, we propose a  
 50 matrix-variate normal prior whose covariance matrix admits a Kronecker product structure to capture  
 51 the correlations between different neurons. Using tools from convex analysis, we present an efficient  
 52 block coordinate descent algorithm with analytical solutions to optimize the model. Empirically, we  
 53 show the proposed method helps the network converge to local optima with smaller stable ranks and  
 54 spectral norms, and we verify the effectiveness of the approach on both multiclass classification and  
 55 multitask regression problems with various network structures.

## 56 2 Preliminary

57 **Notation and Setup** We use lowercase letter to represent scalar and lowercase bold letter to denote  
 58 vector. Capital letter, e.g.,  $X$ , is reserved for matrix. Calligraphic letter, such as  $\mathcal{D}$ , is used to denote  
 59 set. We write  $\text{Tr}(A)$  as the trace of a matrix  $A$ ,  $\det(A)$  as the determinant of  $A$  and  $\text{vec}(A)$  as  
 60  $A$ 's vectorization by column.  $[n]$  is used to represent the set  $\{1, \dots, n\}$  for any integer  $n$ . Other  
 61 notations will be introduced whenever needed. Suppose we have access to a training set  $\mathcal{D}$  of  $n$  pairs  
 62 of data instances  $(\mathbf{x}_i, y_i), i \in [n]$ . We consider the supervised learning setting where  $\mathbf{x}_i \in \mathcal{X} \subseteq \mathbb{R}^d$   
 63 and  $y_i \in \mathcal{Y}$ . Let  $p(y | \mathbf{x}, \mathbf{w})$  be the conditional distribution of  $y$  given  $\mathbf{x}$  with parameter  $\mathbf{w}$ . The  
 64 parametric form of the conditional distribution is assumed be known. In this paper, we assume the  
 65 model parameter  $\mathbf{w}$  is sampled from a prior distribution  $p(\mathbf{w} | \theta)$  with hyperparameter  $\theta$ . On the  
 66 other hand, given  $\mathcal{D}$ , the posterior distribution of  $\mathbf{w}$  is denoted by  $p(\mathbf{w} | \mathcal{D}, \theta)$ .

67 **The Empirical Bayes Method** To compute the predictive distribution, we need access to the value  
 68 of the hyperparameter  $\theta$ . However, complete information about the hyperparameter  $\theta$  is usually not  
 69 available in practice. To this end, empirical Bayes method [1, 9, 10, 12, 39] proposes to estimate  $\theta$   
 70 from the data directly using the marginal distribution:

$$\hat{\theta} = \arg \max_{\theta} p(\mathcal{D} | \theta) = \arg \max_{\theta} \int p(\mathcal{D} | \mathbf{w}) \cdot p(\mathbf{w} | \theta) d\mathbf{w}. \quad (1)$$

71 Under specific choice of the likelihood function  $p(\mathbf{x}, y | \mathbf{w})$  and the prior distribution  $p(\mathbf{w} | \theta)$ , e.g.,  
 72 conjugate pairs, we can solve the above integral in closed form. In certain cases we can even obtain  
 73 an analytic solution of  $\hat{\theta}$ , which can then be plugged into the prior distribution. At a high level, by  
 74 learning the hyperparameter  $\theta$  in the prior distribution directly from data, the empirical Bayes method  
 75 provides us a principled and data-dependent way to obtain an estimator of  $\mathbf{w}$ . In fact, when both the  
 76 prior and the likelihood functions are normal, it has been formally shown that the empirical Bayes  
 77 estimators, e.g., the James-Stein estimator [23] and the Efron-Morris estimator [11], dominate the  
 78 classic maximum likelihood estimator (MLE) in terms of quadratic loss for every choice of the model  
 79 parameter  $\mathbf{w}$ . At a colloquial level, the success of the empirical Bayes method can be attributed to  
 80 the effect of “*borrowing statistical strength*” [8], which also makes it a powerful tool in multitask  
 81 learning [30, 46] and meta-learning [15].

## 82 3 Learning with Adaptive Regularization

83 In this section we first propose an adaptive regularization (AdaReg) method, which is inspired by the  
 84 empirical Bayes method, for learning neural networks. We then combine our observation in Sec. 1  
 85 to develop an efficient adaptive learning algorithm with matrix-variate normal prior. Through our  
 86 derivation, we provide several connections and interpretations with other learning paradigms.

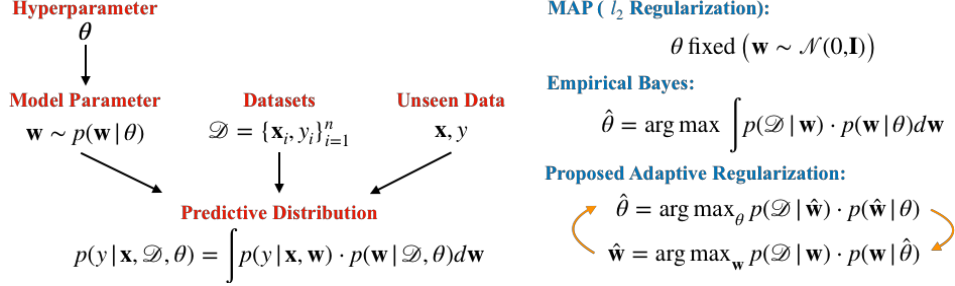


Figure 1: Illustration for Bayes/ Empirical Bayes, and our proposed adaptive regularization.

### 87 3.1 The Proposed Adaptive Regularization

88 When the likelihood function  $p(\mathcal{D} | \mathbf{w})$  is implemented as a neural network, the marginalization in (1)  
 89 over model parameter  $\mathbf{w}$  cannot be computed exactly. Nevertheless, instead of performing expensive  
 90 Monte-Carlo simulation, we propose to estimate both the model parameter  $\mathbf{w}$  and the hyperparameter  
 91  $\theta$  in the prior simultaneously from the joint distribution  $p(\mathcal{D}, \mathbf{w} | \theta) = p(\mathcal{D} | \mathbf{w}) \cdot p(\mathbf{w} | \theta)$ .  
 92 Specifically, given an estimate  $\hat{\mathbf{w}}$  of the model parameter, by maximizing the joint distribution w.r.t.  
 93  $\theta$ , we can obtain  $\hat{\theta}$  as an approximation of the maximum marginal likelihood estimator. As a result,  
 94 we can use  $\hat{\theta}$  to further refine the estimate  $\hat{\mathbf{w}}$  by maximizing the posterior distribution as follows:

$$\hat{\mathbf{w}} \leftarrow \max_{\mathbf{w}} p(\mathbf{w} | \mathcal{D}) = \max_{\mathbf{w}} p(\mathcal{D} | \mathbf{w}) \cdot p(\mathbf{w} | \hat{\theta}). \quad (2)$$

95 The maximizer of (2) can in turn be used in an updated joint distribution. Formally, we can define the  
 96 following optimization problem that characterizes our Adaptive Regularization (AdaReg) framework:  
 97

$$\max_{\mathbf{w}} \max_{\theta} \log p(\mathcal{D} | \mathbf{w}) + \log p(\mathbf{w} | \theta). \quad (3)$$

98 It is worth connecting the optimization problem (3) to the classic maximum a posteriori (MAP)  
 99 inference and also discuss their difference. If we drop the inner optimization over the hyperparameter  
 100  $\theta$  in the prior distribution. Then for any fixed value  $\hat{\theta}$ , (3) reduces to MAP with the prior defined by  
 101 the specific choice of  $\hat{\theta}$ , and the maximizer  $\hat{\mathbf{w}}$  corresponds to the mode of the posterior distribution  
 102 given by  $\hat{\theta}$ . From this perspective, the optimization problem in (3) actually defines a series of MAP  
 103 inference problems, and the sequence  $\{\hat{\mathbf{w}}_j(\hat{\theta}_j)\}_j$  defines a solution path towards the final model  
 104 parameter. On the algorithmic side, the optimization problem (3) also suggests a natural block  
 105 coordinate descent algorithm where we alternatively optimize over  $\mathbf{w}$  and  $\theta$  until the convergence of  
 106 the objective function. An illustration of the framework is shown in Fig. 1.

### 107 3.2 Neural Network with Matrix-Normal Prior

108 Inspired by the observation from Sec. 1, we propose to define a matrix-variate normal distribution [16]  
 109 over the connection weight matrix  $W$ :  $W \sim \mathcal{MN}(0_{p \times d}, \Sigma_r, \Sigma_c)$ , where  $\Sigma_r \in \mathbb{S}_{++}^p$  and  $\Sigma_c \in \mathbb{S}_{++}^d$   
 110 are the row and column covariance matrices, respectively.<sup>1</sup> Equivalently, one can understand the  
 111 matrix-variate normal distribution over  $W$  as a multivariate normal distribution with a Kronecker  
 112 product covariance structure over  $\text{vec}(W)$ :  $\text{vec}(W) \sim \mathcal{N}(0_{p \times d}, \Sigma_c \otimes \Sigma_r)$ . It is then easy to check  
 113 that the marginal prior distributions over the row and column vectors of  $W$  are given by:

$$W_{i:} \sim \mathcal{N}(\mathbf{0}_d, [\Sigma_r]_{ii} \cdot \Sigma_c), \quad W_{:j} \sim \mathcal{N}(\mathbf{0}_p, [\Sigma_c]_{jj} \cdot \Sigma_r).$$

114 We point out that the Kronecker product structure of the covariance matrix exactly captures our prior  
 115 about the connection matrix  $W$ : the fan-in/fan-out of neurons in the same layer (row/column vectors  
 116 of  $W$ ) are correlated with the same correlation matrix in the prior, and they only differ at the scales.

117 For illustration purpose, let us consider the simple feed-forward network discussed in Sec. 1. Consider  
 118 a reparametrization of the model by defining  $\Omega_r := \Sigma_r^{-1}$  and  $\Omega_c := \Sigma_c^{-1}$  to be the corresponding  
 119 precision matrices and plug in the prior distribution into the our AdaReg framework (see (3)). After

<sup>1</sup>The probability density function is given by  $p(W | \Sigma_r, \Sigma_c) = \frac{\exp(-\text{Tr}(\Sigma_r^{-1} W \Sigma_c^{-1} W^T)/2)}{(2\pi)^{pd/2} \det(\Sigma_r)^{d/2} \det(\Sigma_c)^{p/2}}$ .

120 routine algebraic simplifications, we reach the following concrete optimization problem:

$$\min_{W, \mathbf{a}} \min_{\Omega_r, \Omega_c} \frac{1}{2n} \sum_{i \in [n]} (\hat{y}(\mathbf{x}_i; W, \mathbf{a}) - y_i)^2 + \lambda \|\Omega_r^{1/2} W \Omega_c^{1/2}\|_F^2 - \lambda (d \log \det(\Omega_r) + p \log \det(\Omega_c))$$

$$\text{subject to } uI_p \preceq \Omega_r \preceq vI_p, uI_d \preceq \Omega_c \preceq vI_d \quad (4)$$

121 where  $\lambda$  is a constant that only depends on  $p$  and  $d$ ,  $0 < u \leq v$  and  $uv = 1$ . Note that the constraint  
 122 is necessary to guarantee the feasible set to be compact so that the optimization problem is well  
 123 formulated and a minimum is attainable.<sup>2</sup> It is not hard to show that in general the optimization  
 124 problem (4) is not jointly convex in terms of  $\{\mathbf{a}, W, \Omega_r, \Omega_c\}$ , and this holds even if the activation  
 125 function is linear. However, as we will show later, for any fixed  $\mathbf{a}, W$ , the reparametrization makes  
 126 the partial optimization over  $\Omega_r$  and  $\Omega_c$  bi-convex. More importantly, we can derive an efficient  
 127 algorithm that finds the optimal  $\Omega_r(\Omega_c)$  for any fixed  $\mathbf{a}, W, \Omega_c(\Omega_r)$  in  $O(\max\{d^3, p^3\})$  time with  
 128 closed form solutions. This allows us to apply our algorithm to networks of large sizes, where  
 129 a typical hidden layer can contain thousands of nodes. Note that this is in contrast to solving a  
 130 general semi-definite programming (SDP) problem using black-box algorithm, e.g., the interior-point  
 131 method [35], which is computationally intensive and hard to scale to networks with moderate sizes.  
 132 Before we delve into the details on solving (4), it is instructive to discuss some of its connections and  
 133 differences to other learning paradigms.

134 **Maximum-A-Posteriori Estimation.** Essentially, for model parameter  $W$ , (4) defines a sequence of  
 135 MAP problems where each MAP is indexed by the pair of precision matrices  $(\Omega_r^{(t)}, \Omega_c^{(t)})$  at iteration  $t$ .  
 136 Equivalently, at each stage of the optimization, we can interpret (4) as placing a matrix variate normal  
 137 prior on  $W$  where the precision matrix in the prior is given by  $\Omega_r^{(t)} \otimes \Omega_c^{(t)}$ . From this perspective, if  
 138 we fix  $\Omega_r^{(t)} = I_p$  and  $\Omega_c^{(t)} = I_d, \forall t$ , then (4) naturally reduces to learning with  $\ell_2$  regularization [26].  
 139 More generally, for non-diagonal precision matrices, the regularization term for  $W$  becomes:

$$\|\Omega_r^{1/2} W \Omega_c^{1/2}\|_F^2 = \|\text{vec}(\Omega_r^{1/2} W \Omega_c^{1/2})\|_2^2 = \|(\Omega_c^{1/2} \otimes \Omega_r^{1/2}) \text{vec}(W)\|_2^2,$$

140 and this is exactly the Tikhonov regularization [13] imposed on  $W$  where the Tikhonov matrix  $\Gamma$  is  
 141 given by  $\Gamma := \Omega_c^{1/2} \otimes \Omega_r^{1/2}$ . But instead of manually designing the regularization matrix  $\Gamma$  to improve  
 142 the conditioning of the estimation problem, we propose to also learn both precision matrices (so  $\Gamma$  as  
 143 well) from data. From an algorithmic perspective,  $\Gamma^T \Gamma = \Omega_c \otimes \Omega_r$  serves as a preconditioning matrix  
 144 w.r.t. model parameter  $W$  to reshape the gradient according to the geometry of the data [7, 17, 18].

145 **Volume Minimization.** Let us consider the  $\log \det(\cdot)$  function over the positive definite cone. It  
 146 is well known that the log-determinant function is concave [3]. Hence for any pair of matrices  
 147  $A_1, A_2 \in \mathbb{S}_{++}^m$ , the following inequality holds:

$$\log \det(A_1) \leq \log \det(A_2) + \langle \nabla \log \det(A_2), A_1 - A_2 \rangle = \log \det(A_2) + \text{Tr}(A_2^{-1} A_1) - m. \quad (5)$$

148 Applying the above inequality twice by fixing  $A_1 = W \Omega_c W^T / 2d, A_2 = \Sigma_r$  and  $A_1 =$   
 149  $W^T \Omega_r W / 2p, A_2 = \Sigma_c$  respectively leads to the following inequalities:

$$d \log \det(W \Omega_c W^T / 2d) \leq -d \log \det(\Omega_r) + \frac{1}{2} \text{Tr}(\Omega_r W \Omega_c W^T) - dp,$$

$$p \log \det(W^T \Omega_r W / 2p) \leq -p \log \det(\Omega_c) + \frac{1}{2} \text{Tr}(\Omega_r W \Omega_c W^T) - dp.$$

150 Realize  $\text{Tr}(\Omega_r W \Omega_c W^T) = \|\Omega_r^{1/2} W \Omega_c^{1/2}\|_F^2$ . Summing the above two inequalities leads to:

$$d \log \det(W \Omega_c W^T) + p \log \det(W^T \Omega_r W) \leq \|\Omega_r^{1/2} W \Omega_c^{1/2}\|_F^2 - (d \log \det(\Omega_r) + p \log \det(\Omega_c)) + c, \quad (6)$$

151 where  $c$  is a constant that only depends on  $d$  and  $p$ . Recall that  $|\det(A^T A)|$  computes the squared  
 152 volume of the parallelepiped spanned by the column vectors of  $A$ . Hence (6) gives us a natural  
 153 interpretation of the objective function in (4): the regularizer essentially upper bounds the log-volume  
 154 of the two parallelepipeds spanned by the row and column vectors of  $W$ . But instead of measuring the  
 155 volume using standard Euclidean inner product, it also takes into account the local curvatures defined  
 156 by  $\Sigma_r$  and  $\Sigma_c$ , respectively. For vectors with fixed lengths, the volume of the parallelepiped spanned  
 157 by them becomes smaller when they are more linearly correlated, either positively or negatively. At a  
 158 colloquial level, this means that the regularizer in (4) forces fan-in/fan-out of neurons at the same  
 159 layer to be either positively or negatively correlated with each other, and this corresponds exactly to  
 160 the effect of sharing statistical strengths.

<sup>2</sup>The constraint  $uv = 1$  is only for the ease of presentation in the following part and can be readily removed.

---

**Algorithm 1** Block Coordinate Descent for Adaptive Regularization
 

---

**Input:** Initial value  $\phi^{(0)} := \{\mathbf{a}^{(0)}, W^{(0)}\}$ ,  $\Omega_r^{(0)} \in \mathbb{S}_{++}^p$  and  $\Omega_c^{(0)} \in \mathbb{S}_{++}^d$ , first-order optimization algorithm  $\mathfrak{A}$ .

- 1: **for**  $t = 1, \dots, \infty$  until convergence **do**
- 2:   Fix  $\Omega_r^{(t-1)}, \Omega_c^{(t-1)}$ , optimize  $\phi^{(t)}$  by backpropagation and algorithm  $\mathfrak{A}$
- 3:    $\Omega_r^{(t)} \leftarrow \text{INVTHRESHOLD}(W^{(t)}\Omega_c^{(t-1)}W^{(t)T}, d, u, v)$
- 4:    $\Omega_c^{(t)} \leftarrow \text{INVTHRESHOLD}(W^{(t)T}\Omega_r^{(t)}W^{(t)}, p, u, v)$
- 5: **end for**
- 6: **procedure**  $\text{INVTHRESHOLD}(\Delta, m, u, v)$
- 7:   Compute SVD:  $Q\text{diag}(\mathbf{r})Q^T = \text{SVD}(\Delta)$
- 8:   Hard thresholding  $\mathbf{r}' \leftarrow \mathbb{T}_{[u,v]}(m/\mathbf{r})$
- 9:   **return**  $Q\text{diag}(\mathbf{r}')Q^T$
- 10: **end procedure**

---

### 161 3.3 The Algorithm

162 In this section we describe a block coordinate descent algorithm to optimize the objective function  
 163 in (4) and detail how to efficiently solve the matrix optimization subproblems in closed form using  
 164 tools from convex analysis. Due to space limit, we defer proofs and detailed derivation to appendix.  
 165 Given a pair of constants  $0 < u \leq v$ , we define the following thresholding function  $\mathbb{T}_{[u,v]}(x)$ :

$$\mathbb{T}_{[u,v]}(x) := \max\{u, \min\{v, x\}\}. \quad (7)$$

166 We summarize our block coordinate descent algorithm to solve (4) in Alg. 1. In each iteration, Alg. 1  
 167 takes a first-order algorithm  $\mathfrak{A}$ , e.g., the stochastic gradient descent, to optimize the parameters of the  
 168 neural network by backpropagation. It then proceeds to compute the optimal solutions for  $\Omega_r$  and  $\Omega_c$   
 169 using  $\text{INVTHRESHOLD}$  as a sub-procedure. Alg. 1 terminates when a stationary point is found.

170 We now proceed to show that the procedure  $\text{INVTHRESHOLD}$  finds the optimal solution given all the  
 171 other variables fixed. Due to the symmetry between  $\Omega_r$  and  $\Omega_c$  in (4), we will only prove this for  $\Omega_r$ ,  
 172 and similar arguments can be applied to  $\Omega_c$  as well. Fix both  $W$ ,  $\Omega_c$  and ignore all the terms that do  
 173 not depend on  $\Omega_r$ , the sub-problem on optimizing  $\Omega_r$  becomes:

$$\min_{\Omega_r} \text{Tr}(\Omega_r W \Omega_c W^T) - d \log \det(\Omega_r), \quad \text{subject to } uI_p \preceq \Omega_r \preceq vI_p. \quad (8)$$

174 It is not hard to show that the optimization problem (8) is convex. Define the constraint set  
 175  $\mathcal{C} := \{A \in \mathbb{S}_{++}^p \mid uI_p \preceq A \preceq vI_p\}$  and the indicator function  $\mathbb{I}_{\mathcal{C}}(A) = 0$  iff  $A \in \mathcal{C}$  else  
 176  $\infty$ . Given the convexity of (8), we can use the indicator function to first transform (8) into an  
 177 unconstrained one and use the first-order optimality condition to characterize the optimal solu-  
 178 tion:  $0 \in \partial \left( \frac{1}{d} \text{Tr}(\Omega_r W \Omega_c W^T) - \log \det(\Omega_r) + \mathbb{I}_{\mathcal{C}}(\Omega_r) \right) = W \Omega_c W^T / d - \Omega_r^{-1} + \mathcal{N}_{\mathcal{C}}(\Omega_r)$ , where  
 179  $\mathcal{N}_{\mathcal{C}}(A) := \{B \in \mathbb{S}^p \mid \text{Tr}(B^T(Z - A)) \leq 0, \forall Z \in \mathcal{C}\}$  is the normal cone w.r.t.  $\mathcal{C}$  at  $A$ . With the help  
 180 of Lemma 1 in appendix, equivalently, we have  $\Omega_r^{-1} - W \Omega_c W^T / d \in \mathcal{N}_{\mathcal{C}}(\Omega_r)$ . Geometrically, this  
 181 means that the optimum  $\Omega_r^{-1}$  is the Euclidean projection of  $W \Omega_c W^T / d$  onto  $\mathcal{C}$ . Hence in order to  
 182 solve (8), it suffices if we can solve the following Euclidean projection problem efficiently, where  
 183  $\widetilde{\Omega}_r \in \mathbb{S}^p$  is a real symmetric matrix:

$$\min_{\Omega_r} \|\Omega_r - \widetilde{\Omega}_r\|_F^2, \quad \text{subject to } uI_p \preceq \Omega_r \preceq vI_p. \quad (9)$$

184 The following theorem characterizes the optimal solution to the above Euclidean projection problem:

185 **Theorem 1.** Let  $\widetilde{\Omega}_r \in \mathbb{S}^p$  with eigendecomposition as  $\widetilde{\Omega}_r = Q\Lambda Q^T$  and  $\text{Proj}_{\mathcal{C}}(\cdot)$  be the Euclidean  
 186 projection operator onto  $\mathcal{C}$ , then  $\text{Proj}_{\mathcal{C}}(\widetilde{\Omega}_r) = Q\mathbb{T}_{[u,v]}(\Lambda)Q^T$ .

187 **Corollary 1.** Let  $W \Omega_c W^T$  be eigendecomposed as  $Q\text{diag}(\mathbf{r})Q^T$ , then the optimal solution to (8) is  
 188 given by  $Q\mathbb{T}_{[u,v]}(d/\mathbf{r})Q^T$ .

189 Similar arguments can be made to derive the solution for  $\Omega_c$  in (4). The final algorithm is very  
 190 simple as it only contains one SVD, hence its time complexity is  $O(\max\{d^3, p^3\})$ . Note that the total  
 191 number of parameters in the network is at least  $\Omega(dp)$ , hence the algorithm is efficient as it scales  
 192 sub-quadratically in terms of number of parameters in the network.

Table 1: Explained variance of different methods on 7 regression tasks from the SARCOS dataset.

Method	1st	2nd	3rd	4th	5th	6th	7th
<b>MTL</b>	0.4418	0.3472	0.5222	0.5036	0.6024	0.4727	0.5298
<b>MTL-Dropout</b>	0.4413	0.3271	0.5202	0.5063	0.6036	0.4711	0.5345
<b>MTL-BN</b>	0.4768	0.3770	0.5396	0.5216	0.6117	0.4936	0.5479
<b>MTL-DeCoV</b>	0.4027	0.3137	0.4703	0.4515	0.5229	0.4224	0.4716
<b>MTL-AdaReg</b>	<b>0.4769</b>	<b>0.3969</b>	<b>0.5485</b>	<b>0.5308</b>	<b>0.6202</b>	<b>0.5085</b>	<b>0.5561</b>

## 193 4 Experiments

194 In this section we demonstrate the effectiveness of AdaReg in learning practical deep neural networks  
 195 on real-world datasets. We report generalization, optimization as well as stability results.

### 196 4.1 Experimental Setup

197 **Multiclass Classification (MNIST & CIFAR10):** In this experiment, we show that AdaReg provides  
 198 an effective regularization on the network parameters. To this end, we use a convolutional neural  
 199 network as our baseline model. To show the effect of regularization, we gradually increase the  
 200 training set size. In MNIST we use the step from 60 to 60,000 (11 different experiments) and in  
 201 CIFAR10 we consider the step from 5,000 to 50,000 (10 different experiments). For each training  
 202 set size, we repeat the experiments for 10 times. The mean along with its standard deviation are  
 203 shown as the statistics. Moreover, since both the optimization and generalization of neural networks  
 204 are sensitive to the size of minibatches [14, 24], we study two minibatch settings for 256 and 2048,  
 205 respectively. In our method, we place a matrix-variate normal prior over the weight matrix of the last  
 206 softmax layer, and we use Alg. 1 to optimize both the model weights and two covariance matrices.

207 **Multitask Regression (SARCOS):** SARCOS relates to an inverse dynamics problem for a seven  
 208 degree-of-freedom (DOF) SARCOS anthropomorphic robot arm [44]. The goal of this task is to  
 209 map from a 21-dimensional input space (7 joint positions, 7 joint velocities, 7 joint accelerations) to  
 210 the corresponding 7 joint torques. Hence there are 7 tasks and the inputs are shared among all the  
 211 tasks. The training set and test set contain 44,484 and 4,449 examples, respectively. Again, we apply  
 212 AdaReg on the last layer weight matrix, where each row corresponds to a separate task vector.

213 We compare AdaReg with classic regularization methods in the literature, including weight decay,  
 214 dropout [42], batch normalization (BN) [22] and the DeCov method [6]. We also note that we  
 215 fix all the hyperparameters such as learning rate to be the same for all the methods. We report  
 216 evaluation metrics on test set as a measure of generalization. To understand how the proposed  
 217 adaptive regularization helps in optimization, we visualize the trajectory of the loss function during  
 218 training. Lastly, we also present the inferred correlation of the weight matrix for qualitative study.

### 219 4.2 Results and Analysis

220 **Multiclass Classification (MNIST & CIFAR10):** Results on the multiclass classification for dif-  
 221 ferent training sizes are show in Fig. 2. For both MNIST and CIFAR10, we find AdaReg, Weight  
 222 Decay, and Dropout are the effective regularization methods, while Batch Normalization and DeCov  
 223 vary in different settings. Batch Normalization suffers from large batch size in CIFAR10 (comparing  
 224 Fig. 2 (c) and (d)) but is not sensitive to batch size in MNIST (comparing Fig. 2 (a) and (b)). The  
 225 performance deterioration in large batch size of Batch Normalization is also observed by [21]. DeCov,  
 226 on the other hand, improves the generalization in MNIST with batch size 256 (see Fig. 2 (a)), while  
 227 it demonstrates only comparable or even worse performance in other settings. To conclude, as  
 228 training set size grows, AdaReg consistently performs better generalization as comparing to other  
 229 regularization methods. We also note that AdaReg is not sensitive to the size of minibatches while  
 230 most of the methods suffer from large minibatches. In appendix, we show the combination of AdaReg  
 231 with other generalization methods can usually lead to even better results.

232 **Multitask Regression (SARCOS):** In this experiment we are interested in investigating whether  
 233 AdaReg can lead to better generalization for multiple related regression problems. To do so, we  
 234 report the explained variance as a normalized metric, e.g., one minus the ratio between mean squared  
 235 error and the variance of different methods in Table 1. The larger the explained variance, the better

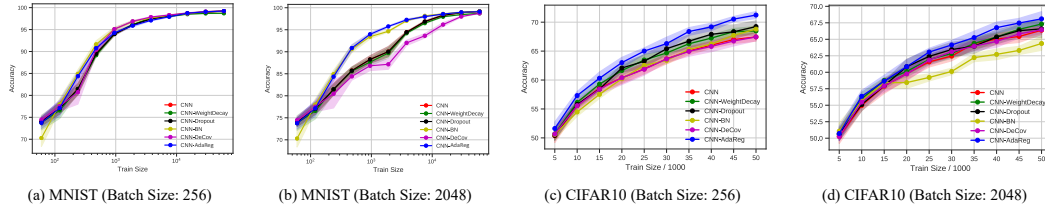


Figure 2: Generalization performance on MNIST and CIFAR10. AdaReg improves generalization under both minibatch settings.

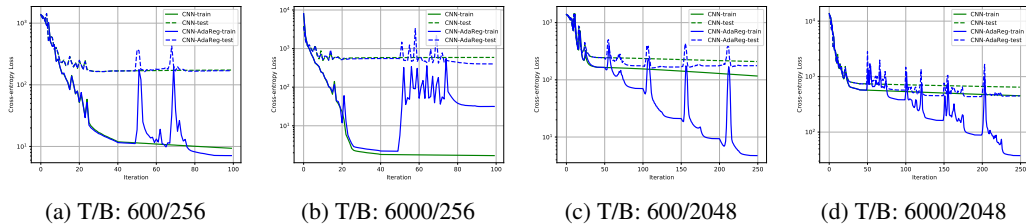


Figure 3: Optimization trajectory of AdaReg on MNIST with training size/batch size on training and test sets. AdaReg helps to converge to better local optima. Note the log-scale on  $y$ -axis.

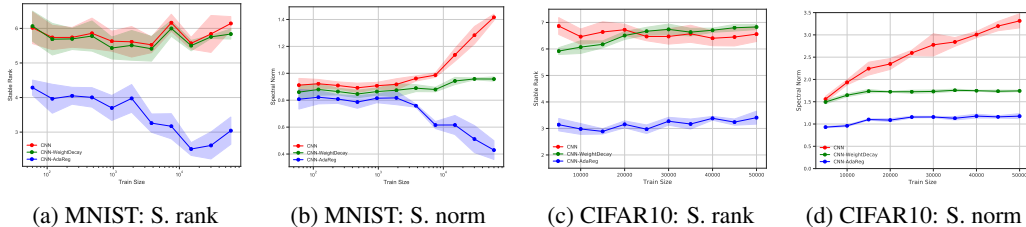
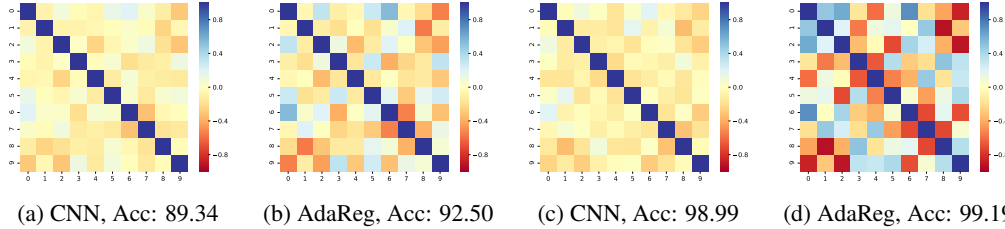


Figure 4: Comparisons of stable ranks (S. rank) and spectral norms (S. norm) from different methods on MNIST and CIFAR10.  $x$ -axis corresponds to the training size.

236 the predictive performance. In this case we observe a consistent improvement of AdaReg over other  
 237 competitors on all the 7 regression tasks. We would like to emphasize that all the experiments  
 238 share exactly the same experimental protocol, including network structure, optimization algorithm,  
 239 training iteration, etc, so that the performance differences can only be explained by different ways of  
 240 regularizations. For better visualization, we also plot the result in appendix.

241 **Optimization:** It has recently been empirically shown that BN helps optimization not by reducing  
 242 internal covariate shift, but instead by smoothing the landscape of the loss function [40]. To understand  
 243 how AdaReg improves generalization, in Fig. 3, we plot the values of the cross entropy loss function  
 244 on both the training and test sets during optimization using Alg. 1. The experiment is performed  
 245 in MNIST with batch size 256/2048. In this experiment, we fix the number of outer loop to be 2/5  
 246 and each block optimization over network weights contains 50 epochs. Because of the stochastic  
 247 optimization over model weights, we can see several unstable peaks in function value around iteration  
 248 50 when trained with AdaReg, which corresponds to the transition phase between two consecutive  
 249 outer loops with different row/column covariance matrices. In all the cases AdaReg converges to  
 250 better local optima of the loss landscape, which lead to better generalization on the test set as well  
 251 because they have smaller loss values on the test set when compared with training without AdaReg.

252 **Stable rank and spectral norm:** Given a matrix  $W$ , the stable rank of  $W$ , denoted as  $\text{srnk}(W)$ , is  
 253 defined as  $\text{srnk}(W) := \|W\|_F^2 / \|W\|_2^2$ . As its name suggests, the stable rank is more stable than  
 254 the rank because it is largely unaffected by tiny singular values. It has recently been shown [37,  
 255 Theorem 1] that the generalization error of neural networks crucially depends on both the stable ranks  
 256 and the spectral norms of connection matrices in the network. Specifically, it can be shown that the  
 257 generalization error is upper bounded by  $O(\sqrt{\prod_{j=1}^L \|W_j\|_2^2 \sum_{j=1}^L \text{srnk}(W_j) / n})$ , where  $L$  is the  
 258 number of layers in the network. Essentially, this upper bound suggests that smaller spectral norm  
 259 (smoother function mapping) and stable rank (skewed spectrum) leads to better generalization.



(a) CNN, Acc: 89.34    (b) AdaReg, Acc: 92.50    (c) CNN, Acc: 98.99    (d) AdaReg, Acc: 99.19  
 Figure 5: Correlation matrix of the weight matrix in the softmax layer. The left two correspond to dataset with training size 600 and the right two with size 60,000. Acc means the test set accuracy.

260 To understand why AdaReg improves generalization, in Fig. 4, we plot both the stable rank and the  
 261 spectral norm of the weight matrix in the last layer of the CNNs used in our MNIST and CIFAR10  
 262 experiments. We compare 3 methods: CNN without any regularization, CNN trained with weight  
 263 decay and CNN with AdaReg. For each setting we repeat the experiments for 5 times, and we plot  
 264 the mean along with its standard deviation. From Fig. 4a and Fig. 4c it is clear that AdaReg leads to a  
 265 significant reduction in terms of the stable rank when compared with weight decay, and this effect  
 266 is consistent in all the experiments with different training size. Similarly, in Fig. 4b and Fig. 4d we  
 267 plot the spectral norm of the weight matrix. Again, both weight decay and AdaReg help reduce the  
 268 spectral norm in all settings, but AdaReg plays a more significant role than the usual weight decay.  
 269 Combining the experiments with the generalization upper bound introduced above, we can see that  
 270 training with AdaReg leads to an estimator of  $W$  that has lower stable rank and smaller spectral norm,  
 271 which explains why it achieves a better generalization performance. Furthermore, this observation  
 272 holds on the SARCOS datasets as well, and we show the results in the appendix.

273 **Correlation Matrix:** To verify that AdaReg imposes the effect of “sharing statistical strength”  
 274 during training, we visualize the weight matrix of the softmax layer by computing the corresponding  
 275 correlation matrix, as shown in Fig. 5. In Fig. 5, darker color means stronger correlation. We conduct  
 276 two experiments with training size 600 and 60,000 respectively. As we can observe, training with  
 277 AdaReg leads to weight matrix with stronger correlations, and this effect is more evident when the  
 278 training set is large. This is consistent with our analysis of sharing statistical strengths. As a sanity  
 279 check, from Fig. 5 we can also see that similar digits, e.g., 1 and 7, share a positive correlation while  
 280 dissimilar ones, e.g., 1 and 8, share a negative correlation.

## 281 5 Related Work

282 Despite the name, empirical Bayes method is in fact a frequentist approach to obtain estimator with  
 283 favorable properties. On the other hand, truly Bayesian inference would instead put a posterior  
 284 distribution over model weights to characterize the uncertainty during training [2, 20, 32]. However,  
 285 due to the complexity of nonlinear neural networks, analytic posterior is not available, hence strong  
 286 independent assumptions over model weight have to be made in order to achieve computationally  
 287 tractable variational solution. Typically, both the prior and the variational posterior are assumed  
 288 to fully factorize over model weights. As an exception, Louizos and Welling [31], Sun et al. [43]  
 289 seek to learn Bayesian neural nets where they approximate the intractable posterior distribution  
 290 using matrix-variate Gaussian distribution. The prior for weights are still assumed to be known and  
 291 fixed. As a comparison, we use matrix-variate Gaussian as the prior distribution and we learn the  
 292 hyperparameter in the prior from data. Hence our method does not belong to Bayesian neural nets:  
 293 we instead use the empirical Bayes principle to derive adaptive regularization method in order to have  
 294 better generalization, as done in [4, 38].

## 295 6 Conclusion

296 Inspired by empirical Bayes method, we propose an adaptive regularization (AdaReg) with matrix-  
 297 variate normal prior for model parameters in deep neural networks. The prior encourages neurons  
 298 to borrow statistical strength from other neurons during the learning process, and it provides an  
 299 effective regularization when training networks on small datasets. To optimize the model, we design  
 300 an efficient block coordinate descent algorithm to learn both model weights and the covariance  
 301 structures. Empirically, on three datasets we demonstrate that AdaReg improves generalization by  
 302 finding better local optima with smaller spectral norms and stable ranks.

## References

- 303
- 304 [1] José M Bernardo and Adrian FM Smith. Bayesian theory, 2001.
- 305 [2] Charles Blundell, Julien Cornebise, Koray Kavukcuoglu, and Daan Wierstra. Weight uncertainty  
306 in neural networks. *arXiv preprint arXiv:1505.05424*, 2015.
- 307 [3] Stephen Boyd and Lieven Vandenberghe. *Convex optimization*. Cambridge university press,  
308 2004.
- 309 [4] Philip J Brown, James V Zidek, et al. Adaptive multivariate ridge regression. *The Annals of*  
310 *Statistics*, 8(1):64–74, 1980.
- 311 [5] Rich Caruana, Steve Lawrence, and C Lee Giles. Overfitting in neural nets: Backpropagation,  
312 conjugate gradient, and early stopping. In *Advances in neural information processing systems*,  
313 pages 402–408, 2001.
- 314 [6] Michael Cogswell, Faruk Ahmed, Ross Girshick, Larry Zitnick, and Dhruv Batra. Reducing  
315 overfitting in deep networks by decorrelating representations. *arXiv preprint arXiv:1511.06068*,  
316 2015.
- 317 [7] John Duchi, Elad Hazan, and Yoram Singer. Adaptive subgradient methods for online learning  
318 and stochastic optimization. *Journal of Machine Learning Research*, 12(Jul):2121–2159, 2011.
- 319 [8] Bradley Efron. *Large-scale inference: empirical Bayes methods for estimation, testing, and*  
320 *prediction*, volume 1. Cambridge University Press, 2012.
- 321 [9] Bradley Efron and Trevor Hastie. *Computer age statistical inference*, volume 5. Cambridge  
322 University Press, 2016.
- 323 [10] Bradley Efron and Carl Morris. Stein’s estimation rule and its competitors—an empirical Bayes  
324 approach. *Journal of the American Statistical Association*, 68(341):117–130, 1973.
- 325 [11] Bradley Efron and Carl Morris. Stein’s paradox in statistics. *Scientific American*, 236(5):  
326 119–127, 1977.
- 327 [12] Andrew Gelman, John B Carlin, Hal S Stern, David B Dunson, Aki Vehtari, and Donald B  
328 Rubin. *Bayesian data analysis*. CRC press, 2013.
- 329 [13] Gene H Golub, Michael Heath, and Grace Wahba. Generalized cross-validation as a method for  
330 choosing a good ridge parameter. *Technometrics*, 21(2):215–223, 1979.
- 331 [14] Priya Goyal, Piotr Dollár, Ross Girshick, Pieter Noordhuis, Lukasz Wesolowski, Aapo Kyrola,  
332 Andrew Tulloch, Yangqing Jia, and Kaiming He. Accurate, large minibatch sgd: training  
333 imagenet in 1 hour. *arXiv preprint arXiv:1706.02677*, 2017.
- 334 [15] Erin Grant, Chelsea Finn, Sergey Levine, Trevor Darrell, and Thomas Griffiths. Recasting  
335 gradient-based meta-learning as hierarchical bayes. *arXiv preprint arXiv:1801.08930*, 2018.
- 336 [16] Arjun K Gupta and Daya K Nagar. *Matrix variate distributions*. Chapman and Hall/CRC, 2018.
- 337 [17] Vineet Gupta, Tomer Koren, and Yoram Singer. A unified approach to adaptive regularization  
338 in online and stochastic optimization. *arXiv preprint arXiv:1706.06569*, 2017.
- 339 [18] Elad Hazan, Amit Agarwal, and Satyen Kale. Logarithmic regret algorithms for online convex  
340 optimization. *Machine Learning*, 69(2-3):169–192, 2007.
- 341 [19] Kaiming He, Xiangyu Zhang, Shaoqing Ren, and Jian Sun. Deep residual learning for image  
342 recognition. In *Proceedings of the IEEE conference on computer vision and pattern recognition*,  
343 pages 770–778, 2016.
- 344 [20] José Miguel Hernández-Lobato and Ryan Adams. Probabilistic backpropagation for scalable  
345 learning of bayesian neural networks. In *International Conference on Machine Learning*, pages  
346 1861–1869, 2015.

- 347 [21] Elad Hoffer, Itay Hubara, and Daniel Soudry. Train longer, generalize better: closing the  
348 generalization gap in large batch training of neural networks. In *Advances in Neural Information*  
349 *Processing Systems*, pages 1731–1741, 2017.
- 350 [22] Sergey Ioffe and Christian Szegedy. Batch normalization: Accelerating deep network training  
351 by reducing internal covariate shift. *arXiv preprint arXiv:1502.03167*, 2015.
- 352 [23] William James and Charles Stein. Estimation with quadratic loss. In *Proceedings of the fourth*  
353 *Berkeley symposium on mathematical statistics and probability*, volume 1, pages 361–379,  
354 1961.
- 355 [24] Nitish Shirish Keskar, Dheevatsa Mudigere, Jorge Nocedal, Mikhail Smelyanskiy, and Ping  
356 Tak Peter Tang. On large-batch training for deep learning: Generalization gap and sharp minima.  
357 *arXiv preprint arXiv:1609.04836*, 2016.
- 358 [25] Alex Krizhevsky and Geoffrey Hinton. Learning multiple layers of features from tiny images.  
359 2009.
- 360 [26] Anders Krogh and John A Hertz. A simple weight decay can improve generalization. In  
361 *Advances in neural information processing systems*, pages 950–957, 1992.
- 362 [27] Alex Kulesza and Ben Taskar. Learning determinantal point processes. In *Proceedings of the*  
363 *Twenty-Seventh Conference on Uncertainty in Artificial Intelligence*, pages 419–427. AUAI  
364 Press, 2011.
- 365 [28] Alex Kulesza, Ben Taskar, et al. Determinantal point processes for machine learning. *Founda-*  
366 *tions and Trends® in Machine Learning*, 5(2–3):123–286, 2012.
- 367 [29] Yann LeCun, Yoshua Bengio, and Geoffrey Hinton. Deep learning. *nature*, 521(7553):436,  
368 2015.
- 369 [30] Mingsheng Long, Zhangjie Cao, Jianmin Wang, and S Yu Philip. Learning multiple tasks  
370 with multilinear relationship networks. In *Advances in Neural Information Processing Systems*,  
371 pages 1594–1603, 2017.
- 372 [31] Christos Louizos and Max Welling. Structured and efficient variational deep learning with  
373 matrix gaussian posteriors. In *International Conference on Machine Learning*, pages 1708–1716,  
374 2016.
- 375 [32] David JC MacKay. A practical bayesian framework for backpropagation networks. *Neural*  
376 *computation*, 4(3):448–472, 1992.
- 377 [33] Zelda Mariet and Suvrit Sra. Diversity networks: Neural network compression using determi-  
378 nantal point processes. *arXiv preprint arXiv:1511.05077*, 2015.
- 379 [34] James Martens and Roger Grosse. Optimizing neural networks with kronecker-factored ap-  
380 proximate curvature. In *International conference on machine learning*, pages 2408–2417,  
381 2015.
- 382 [35] Sanjay Mehrotra. On the implementation of a primal-dual interior point method. *SIAM Journal*  
383 *on optimization*, 2(4):575–601, 1992.
- 384 [36] Vinod Nair and Geoffrey E Hinton. Rectified linear units improve restricted boltzmann machines.  
385 In *Proceedings of the 27th international conference on machine learning (ICML-10)*, pages  
386 807–814, 2010.
- 387 [37] Behnam Neyshabur, Srinadh Bhojanapalli, David McAllester, and Nathan Srebro. A pac-  
388 bayesian approach to spectrally-normalized margin bounds for neural networks. *arXiv preprint*  
389 *arXiv:1707.09564*, 2017.
- 390 [38] Samuel D Oman. A different empirical bayes interpretation of ridge and stein estimators.  
391 *Journal of the Royal Statistical Society: Series B (Methodological)*, 46(3):544–557, 1984.
- 392 [39] Herbert Robbins. An empirical bayes approach to statistics. Technical report, Columbia  
393 University, New York City, United States, 1956.

- 394 [40] Shibani Santurkar, Dimitris Tsipras, Andrew Ilyas, and Aleksander Madry. How does batch  
395 normalization help optimization?(no, it is not about internal covariate shift). *arXiv preprint*  
396 *arXiv:1805.11604*, 2018.
- 397 [41] Karen Simonyan and Andrew Zisserman. Very deep convolutional networks for large-scale  
398 image recognition. *arXiv preprint arXiv:1409.1556*, 2014.
- 399 [42] Nitish Srivastava, Geoffrey Hinton, Alex Krizhevsky, Ilya Sutskever, and Ruslan Salakhutdinov.  
400 Dropout: A simple way to prevent neural networks from overfitting. *The Journal of Machine*  
401 *Learning Research*, 15(1):1929–1958, 2014.
- 402 [43] Shengyang Sun, Changyou Chen, and Lawrence Carin. Learning structured weight uncertainty  
403 in bayesian neural networks. In *Artificial Intelligence and Statistics*, pages 1283–1292, 2017.
- 404 [44] Sethu Vijayakumar and Stefan Schaal. Locally weighted projection regression: Incremental  
405 real time learning in high dimensional space. In *Proceedings of the Seventeenth International*  
406 *Conference on Machine Learning*, pages 1079–1086. Morgan Kaufmann Publishers Inc., 2000.
- 407 [45] Guodong Zhang, Shengyang Sun, David Duvenaud, and Roger Grosse. Noisy natural gradient  
408 as variational inference. *arXiv preprint arXiv:1712.02390*, 2017.
- 409 [46] Han Zhao, Otilia Stretcu, Alex Smola, and Geoff Gordon. Efficient multitask feature and  
410 relationship learning. In *Proceedings of the Thirty-Fifth Conference on Uncertainty in Artificial*  
411 *Intelligence*. AUAI Press, 2019.

412 In this appendix we first describe more related work, and then present missing proofs in the main  
 413 section. We also provide detailed description of our experiments.

## 414 A More Related Work

415 Different kinds of regularization approaches have been studied and designed for neural networks,  
 416 e.g., weight decay [26], early stopping [5], Dropout [42] and the more recent DeCov [6] method.  
 417 BN was proposed to reduce the internal covariate shift during training, but recently it has been  
 418 empirically shown to actually smooth the landscape of the loss function [40]. As a comparison, we  
 419 propose AdaReg as an adaptive regularization method, with the aim to reduce overfitting by allowing  
 420 neurons to share statistical strengths. From the optimization perspective, learning the row and column  
 421 covariance matrices help to converge to better local optimum that also generalizes better.

422 The Kronecker factorization assumption has also been applied in the literature of neural networks  
 423 to approximate the Fisher information matrix in second-order optimization methods [34, 45]. The  
 424 main idea here is to approximate the curvature of the loss function’s landscape, in order to achieve  
 425 better convergence speed compared with first-order method while maintaining the tractability of such  
 426 computation.

427 Determinantal point process (DPP) has been previously applied to compress neural networks [33].  
 428 Specifically, a DPP kernel is placed over the activations of neurons from the same layer, and then  
 429 neurons with similar activations over a fixed dataset are merged into a single one. However, it is  
 430 well known that DPPs can capture only negative correlations [27, 28], and as a result they do not  
 431 stimulate neurons to learn from the experience of other neurons. As a comparison, by explicitly  
 432 learning both precision (covariance) matrices, our framework can account for both positive and  
 433 negative correlations among fan-in/fan-out of neurons from the same layer.

## 434 B Detailed Derivation and Proofs of Our Algorithm

435 We first show that the optimization problem (8) is convex:

436 **Proposition 1.** The optimization problem (8) is convex.

437 *Proof.* It is clear that the objective function is convex: the trace term is linear in  $\Omega_r$  and it is well-  
 438 known that the  $\log \det(\cdot)$  is concave in the positive definite cone [3], hence it trivially follows that  
 439  $\text{Tr}(\Omega_r W \Omega_c W^T) - d \log \det(\Omega_r)$  is convex in  $\Omega_r$ .

440 It remains to show that the constraint set is also convex. Let  $\Omega_1, \Omega_2$  be any feasible points, i.e.,  
 441  $uI_p \preceq \Omega_1 \preceq vI_p$  and  $uI_p \preceq \Omega_2 \preceq vI_p$ . Let  $\forall t \in (0, 1)$ , we have:

$$\|t\Omega_1 + (1-t)\Omega_2\|_2 \leq t\|\Omega_1\|_2 + (1-t)\|\Omega_2\|_2 \leq tv + (1-t)v = v,$$

442 where we use  $\|\cdot\|_2$  to denote the spectral norm of a matrix. Now since both  $\Omega_1$  and  $\Omega_2$  are positive  
 443 definite, the spectral norm is also the largest eigenvalue, hence this shows that  $t\Omega_1 + (1-t)\Omega_2 \preceq vI_p$ .

444 To show the other direction, we use the Courant-Fischer characterization of eigenvalues. Let  $\lambda_{\min}(A)$   
 445 denote the minimum eigenvalue of a real symmetric matrix  $A$ , then by the Courant-Fischer min-max  
 446 theorem, we have:

$$\lambda_{\min}(A) := \min_{\mathbf{x} \neq 0, \|\mathbf{x}\|_2=1} \|A\mathbf{x}\|_2.$$

447 For the matrix  $t\Omega_1 + (1-t)\Omega_2$ , let  $\mathbf{x}^*$  be the vector corresponding to the minimum eigenvalue, hence  
 448 we have:

$$\begin{aligned} \lambda_{\min}(t\Omega_1 + (1-t)\Omega_2) &= \min_{\mathbf{x} \neq 0, \|\mathbf{x}\|_2=1} \|(t\Omega_1 + (1-t)\Omega_2)\mathbf{x}\|_2 \\ &= (t\Omega_1 + (1-t)\Omega_2)\mathbf{x}^* \\ &\geq t\lambda_{\min}(\Omega_1) + (1-t)\lambda_{\min}(\Omega_2) \\ &\geq tu + (1-t)u \\ &= u, \end{aligned}$$

449 which also means that  $t\Omega_1 + (1-t)\Omega_2 \succeq uI_p$ , and this completes the proof. ■

450 The following key lemma characterizes the structure of the normal cone:

451 **Lemma 1.** Let  $\Omega_r \in \mathcal{C}$ , then  $\mathcal{N}_{\mathcal{C}}(\Omega_r) = -\mathcal{N}_{\mathcal{C}}(\Omega_r^{-1})$ .

452 *Proof.* Let  $S \in \mathcal{N}_{\mathcal{C}}(\Omega_r)$ . We want to show  $-S \in \mathcal{N}_{\mathcal{C}}(\Omega_r^{-1})$ . By definition of the normal cone, since  
453  $S \in \mathcal{N}_{\mathcal{C}}(\Omega_r)$ , we have:

$$\text{Tr}(SZ) \leq \text{Tr}(S\Omega_r), \quad \forall Z \in \mathcal{C}$$

454 Now realize that  $\Omega_r \in \mathcal{C}$  and  $\mathcal{C}$  is a compact set, it follows  $\Omega_r$  is the solution of the following linear  
455 program:

$$\max \text{Tr}(SZ), \quad \text{subject to } Z \in \mathcal{C}$$

456 Since both  $S$  and  $Z$  are real symmetric matrix, we can decompose them as  $Z := Q_Z \Lambda_Z Q_Z^T$  and  
457  $S := Q_S \Lambda_S Q_S^T$ , where both  $Q_Z, Q_S$  are orthogonal matrices and  $\Lambda_Z, \Lambda_S$  are diagonal matrices with  
458 the corresponding eigenvalues in decreasing order. Plug them into the objective function, we have:

$$\text{Tr}(SZ) = \text{Tr}(Q_S \Lambda_S Q_S^T Q_Z \Lambda_Z Q_Z^T) = \text{Tr}(\Lambda_S Q_S^T Q_Z \Lambda_Z Q_Z^T Q_S).$$

459 Define  $K := Q_S^T Q_Z$  and  $D = K \circ K$ , where we use  $\circ$  to denote the Hadamard product between two  
460 matrices. Since both  $Q_S$  and  $Q_Z$  are orthogonal matrices, we know that  $K$  is also orthogonal, which  
461 implies:

$$\sum_{j=1}^p D_{ij} = 1, \forall i \in [p], \quad \text{and} \quad \sum_{i=1}^p D_{ij} = 1, \forall j \in [p].$$

462 As a result,  $D$  is a doubly stochastic matrix and we can further simplify the objective function as:

$$\text{Tr}(\Lambda_S Q_S^T Q_Z \Lambda_Z Q_Z^T Q_S) = \text{Tr}(\Lambda_S K \Lambda_Z K^T) = \lambda_S^T D \lambda_Z = \sum_{i,j=1}^p \lambda_{S,i} D_{ij} \lambda_{Z,j},$$

463 where  $\lambda_S$  and  $\lambda_Z$  are  $p$  dimensional vectors that contain the eigenvalues of  $S$  and  $Z$  in decreasing  
464 order, respectively. Now for any  $\lambda_S$  and  $\lambda_Z$  in decreasing order, we have:

$$u \sum_{i=1}^p \lambda_{S,i} \leq \sum_{i=1}^p \lambda_{S,i} \lambda_{Z,1+p-i} \leq \sum_{i,j=1}^p \lambda_{S,i} D_{ij} \lambda_{Z,j} \leq \sum_{i=1}^p \lambda_{S,i} \lambda_{Z,i} \leq v \sum_{i=1}^p \lambda_{S,i} \quad (10)$$

465 From (10), in order for  $\Omega_r$  to maximize the linear program, it must hold that  $D = K = I_p$  and all the  
466 eigenvalues of  $\Omega_r$  are  $v$ . But due to the assumption that  $uv = 1$ , in this case we also know that all  
467 the eigenvalues of  $\Omega_r^{-1}$  are  $1/v = u$ , hence  $\Omega_r^{-1}$  also minimizes the above linear program, which  
468 implies:

$$\text{Tr}(S\Omega_r^{-1}) \leq \text{Tr}(SZ), \quad \forall Z \in \mathcal{C} \Leftrightarrow \text{Tr}(-S(Z - \Omega_r^{-1})) \leq 0 \quad \forall Z \in \mathcal{C}.$$

469 In other words, we have  $-S \in \mathcal{N}_{\mathcal{C}}(\Omega_r^{-1})$ . Using exactly the same arguments it is clear to see that the  
470 other direction also holds, hence we have  $\mathcal{N}_{\mathcal{C}}(\Omega_r) = -\mathcal{N}_{\mathcal{C}}(\Omega_r^{-1})$ . ■

471 Based on the previous first-order optimality condition, it is clear to see that Lemma 1 implies  
472  $W\Omega_c W^T/d - \Omega_r^{-1} \in \mathcal{N}_{\mathcal{C}}(\Omega_r^{-1})$ . Geometrically, this means that the optimum  $\Omega_r^{-1}$  is the Euclidean  
473 projection of  $W\Omega_c W^T/d$  onto  $\mathcal{C}$ . Hence we proceed to derive the projection operator:

474 **Theorem 1.** Let  $\widetilde{\Omega}_r \in \mathbb{S}^p$  with eigendecomposition as  $\widetilde{\Omega}_r = Q\Lambda Q^T$  and  $\text{Proj}_{\mathcal{C}}(\cdot)$  be the Euclidean  
475 projection operator onto  $\mathcal{C}$ , then  $\text{Proj}_{\mathcal{C}}(\widetilde{\Omega}_r) = Q\mathbb{T}_{[u,v]}(\Lambda)Q^T$ .

476 *Proof.* Since  $\Omega_r \in \mathcal{C}$  is real and symmetric, we can reparametrize  $\Omega_r$  as  $\Omega_r := U\Lambda_{\Omega_r}U^T$  where  $U$   
477 is an orthogonal matrix and  $\Lambda_{\Omega_r}$  is a diagonal matrix whose entries corresponds to the eigenvalues of  
478  $\Omega_r$ . Recall that  $U$  corresponds to a rigid transformation that preserves length, so we have:

$$\|\Omega_r - \widetilde{\Omega}_r\|_F^2 = \|U\Lambda_{\Omega_r}U^T - UU^T\widetilde{\Omega}_rUU^T\|_F^2 = \|\Lambda_{\Omega_r} - U^T\widetilde{\Omega}_rU\|_F^2 \quad (11)$$

479 Define  $B := U^T\widetilde{\Omega}_rU$ . Now by using the fact that  $\widetilde{\Omega}_r$  can be eigendecomposed as  $\widetilde{\Omega}_r = Q\Lambda Q^T$ , we  
480 can further simplify (11) as:

$$\|\Lambda_{\Omega_r} - U^T\widetilde{\Omega}_rU\|_F^2 = \sum_{i \in [p]} (\Lambda_{\Omega_r,ii} - B_{ii})^2 + \sum_{i \neq j} B_{ij}^2 \geq \sum_{i \in [p]} (\Lambda_{\Omega_r,ii} - B_{ii})^2 \geq \sum_{i \in [p]} (\mathbb{T}_{[u,v]}(B_{ii}) - B_{ii})^2,$$

481 where the last inequality holds because  $u \leq \Lambda_{\Omega_r,ii} \leq v, \forall i \in [p]$ . In order to achieve the first  
482 equality,  $B = U^T\widetilde{\Omega}_rU$  should be a diagonal matrix, which means  $U^T Q = I_p \Leftrightarrow U = Q$ . In this  
483 case,  $\text{diag}(B) = \Lambda$ . To achieve the second equality, simply let  $\Lambda_{\Omega_r} = \mathbb{T}_{[u,v]}(\text{diag}(B)) = \mathbb{T}_{[u,v]}(\Lambda)$ ,  
484 which completes the proof. ■

Table 2: Stable rank and spectral norm on SARCOS.

	Stable Rank	Spectral Norm
MTL	4.48	0.96
MTL-WeightDecay	4.83	0.92
MTL-AdaReg	<b>2.88</b>	<b>0.70</b>

## 485 C More Experiments

486 In this section we first describe the network structures used in our main experiments and present more  
487 experimental results.

### 488 C.1 Network Structures

489 **Multiclass Classification (MNIST & CIFAR10):** We use a convolutional neural network as our  
490 baseline model. The network used in the experiment has the following structure:  $\text{CONV}_{5 \times 5 \times 1 \times 10}$ -  
491  $\text{CONV}_{5 \times 5 \times 10 \times 20}$ - $\text{FC}_{320 \times 50}$ - $\text{FC}_{50 \times 10}$ . The notation  $\text{CONV}_{5 \times 5 \times 1 \times 10}$  denotes a convolutional layer  
492 with kernel size  $5 \times 5$  from depth 1 to 10; the notation  $\text{FC}_{320 \times 50}$  denotes a fully connected layer  
493 with size  $320 \times 50$ . Similarly, CIFAR10 considers the structure:  $\text{CONV}_{5 \times 5 \times 3 \times 10}$ - $\text{CONV}_{5 \times 5 \times 10 \times 20}$ -  
494  $\text{FC}_{500 \times 500}$ - $\text{FC}_{500 \times 500}$ - $\text{FC}_{500 \times 10}$ .

495 **Multitask Regression (SARCOS):** The network structure is given by  $\text{FC}_{21 \times 256}$ - $\text{FC}_{256 \times 100}$ -  
496  $\text{FC}_{100 \times 7}$ .

### 497 C.2 Stable Rank and Spectral Norm on SARCOS

498 We also show the experimental results of stable ranks and spectral norms on the SARCOS dataset.  
499 For the SARCOS dataset, the weight matrix being regularized is of dimension  $100 \times 7$ . Again, we  
500 compare the results using three methods: MTL, MTL-WeightDecay and MTL-AdaReg. As can be  
501 observed from Table 2, compared with the weight decay regularization, AdaReg greatly reduces  
502 both the stable rank and the spectral norm of learned weight matrix, which also helps to explain why  
503 MTL-AdaReg generalizes better compared with MTL and MTL-WeightDecay.

### 504 C.3 Combination

505 As discussed in the main text, combining the proposed AdaReg with BN can further improve the  
506 generalization performance, due to the complementary effects between these two approaches: BN  
507 helps smoothing the landscape of the loss function while AdaReg also changes the curvature via the  
508 row and column covariance matrices (see Fig. 6).

509 On the other hand, we do not observe significant difference when combining AdaReg with Dropout  
510 on this dataset. While we are not clear what is the exact reason for this effect, we conjecture this is  
511 due to the fact that Dropout works as a regularizer that prevents coadaptation while AdaReg instead  
512 encourages neurons to learn from each other.

### 513 C.4 Ablations

514 In all the experiments, the AdaReg algorithm is performed on the softmax layer. Here, we study  
515 the effects of applying AdaReg algorithm in all CONV/FC layers, all CONV layers, all FC layers,  
516 and the last FC layer (i.e., softmax layer). We first discuss how we handle the convolutions in our  
517 AdaReg algorithm. Consider a convolutional layer with {input channel, output channel, kernel width,  
518 kernel height} being  $\{a, b, k_w, k_h\}$ , we vectorize the original 4-D tensor to be a 2-D matrix of size  
519  $ak_w k_h \times b$ . The AdaReg algorithm can therefore be directly applied on this transformed matrix.  
520 Next, we perform the experiment on MNIST with batch size 2048 in Fig. 7. The training set size here  
521 is chosen as  $\{128, 256, 512, 1024, 2048, 4096, 8192, 16384, 32768, 60000\}$ .

522 We find that simply applying the AdaReg algorithm in the softmax layer reaches best generalization  
523 as comparing to applying AdaReg on more layers. The improvement is more obvious when the  
524 training set size is small. We argue that neural networks can be realized as a combination of a complex

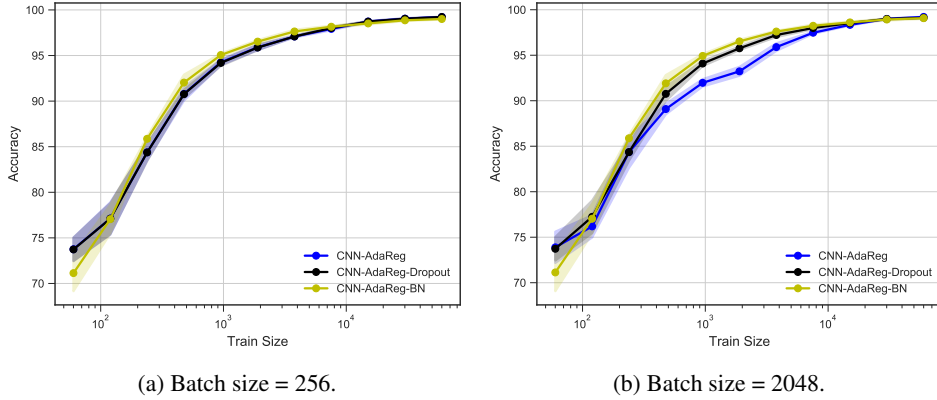


Figure 6: Combine AdaReg with BN and Dropout on MNIST.

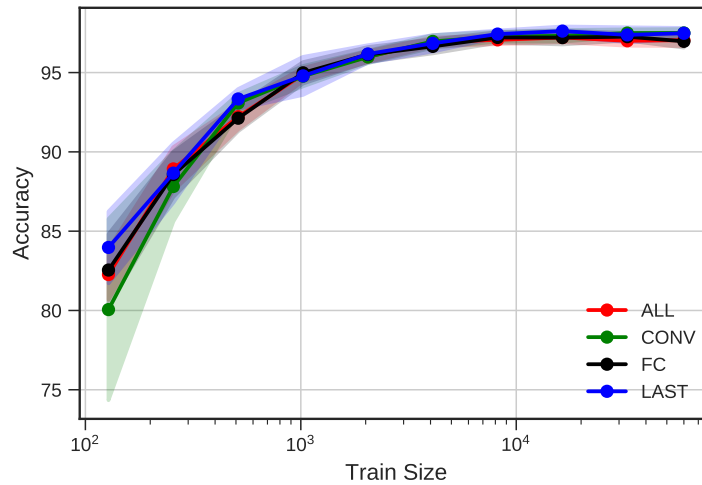


Figure 7: Applying AdaReg on different layers in neural networks for MNIST with batch size 2048.

525 nonlinear transformation (i.e., feature extraction) and a linear model (i.e., softmax layer). Since  
 526 AdaReg represents a correlation learning in the weight matrix, it implies that implicit correlations  
 527 of neurons can also be discovered. In the real world setting, different tasks should be correlated.  
 528 Therefore, applying AdaReg in the linear model shall improve the model performance by discovering  
 529 these tasks correlations. On the contrary, the nonlinear features should be decorrelated for the purpose  
 530 of generalization. Hence, applying AdaReg in previous layers may lead to adversarial effect.

### 531 C.5 Covariance matrices in the prior

532 One byproduct that AdaReg brings to us is the learned row and column covariance matrices, which  
 533 can be used in exploratory data analysis to understand the correlations between learned features and  
 534 different output tasks. To this end, we visualize both the row and column covariance matrices in  
 535 Fig. 8. The two covariance matrices on the first row correspond to the ones learned on a training set  
 536 with 600 instances while the two on the second row are trained with the full dataset on MNIST.

537 From Fig. 8 we can make the following observations: the structure of both covariance matrices  
 538 become more evident when trained with larger dataset, and this is consistent with the Bayesian  
 539 principle because more data provide more evidence. Second, we observe in our experiments that the  
 540 variances of both matrices are small. In fact, the variance of the row covariance matrix  $\Sigma_r$  achieves  
 541 the lower bound limit  $u$  at convergence. Lastly, comparing the row covariance matrix  $\Sigma_r$  in Fig. 8  
 542 with the one computed from model weights in Fig. 5, we can see that both matrices exhibit the same  
 543 correlation patterns, except that the one obtained from model weights are more evident, which is

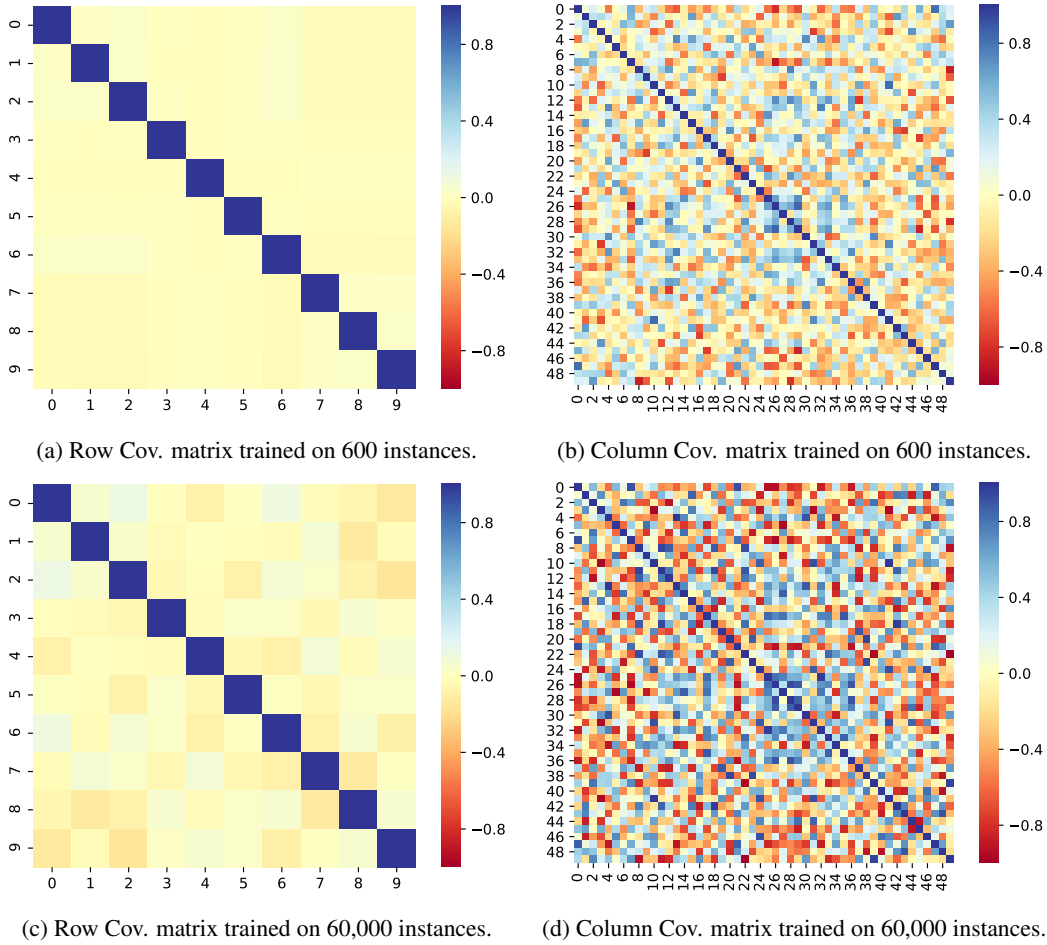


Figure 8: Recovered row covariance matrix  $\Sigma_r$  and column covariance matrix  $\Sigma_c$  in the prior distribution on MNIST.

544 due to the fact that model weights are closer to data evidence than the row covariance matrix in the  
 545 Bayesian hierarchy.

546 On the other hand, the column covariance matrix in Fig. 8 also exhibit rich correlations between the  
 547 learned features, e.g., the neurons in the penultimate layer. Again, with more data, these patterns  
 548 become more evident.

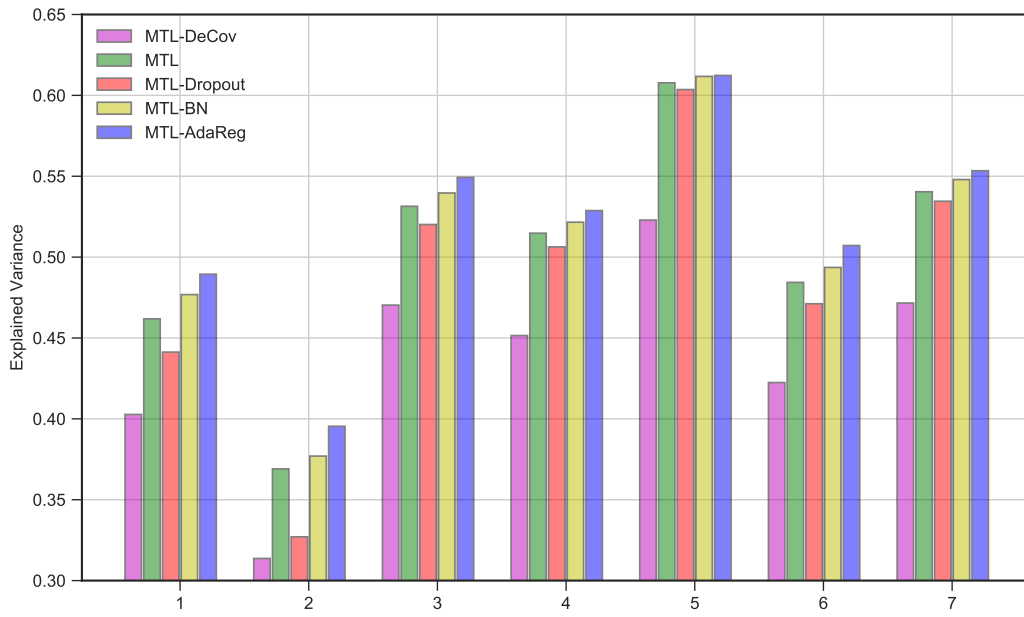


Figure 9: Explained variance of different methods on 7 regression tasks from the SARCOS dataset.